

# Density-Based Histogram Partitioning and Local Equalization for Contrast Enhancement of Images

M. Shakeri, M.-H. Dezfoulian, H. Khotanlou\*

Department of Computer Engineering, Bu-Ali Sina University, Hamedan, Iran.

Receive 10 January 2016; Accepte 08 April 2017

\*Corresponding author: khotanlou@basu.ac.ir (H. Khotanlou).

## Abstract

Histogram Equalization technique is one of the basic methods available in image contrast enhancement. The use of this method in the case of images with uniform gray levels (with a narrow histogram) causes the loss of image details and the natural look of the image. In order to overcome this problem and to have a better image contrast enhancement, a new two-step method is proposed. In the first step, the image histogram is partitioned into some sub-histograms according to the mean value and standard deviation, which is controlled with the PSNR measure. In the second step, each sub-histogram is improved separately and locally with the traditional histogram equalization. Finally, all sub-histograms are combined to obtain the enhanced image. The experimental results show that this method would not only keep the visual details of the histogram but also enhance the image contrast.

**Keywords:** *Contrast Enhancement, Histogram Modification, Image Quality Evaluation, Image Quality Enhancement.*

## 1. Introduction

Image enhancement methods have been widely used in many applications of image processing. Contrast is a main factor in any subjective evaluation of image quality. Contrast enhancement is one of the most important areas in the image processing for human and machine vision, and many techniques have been proposed for contrast enhancement and applied to problems in image processing. This area has great applications in medical image processing, remote sensing [1-4], digital photography [5], video surveillance systems [6], recovery of underwater visibility [7], and face recognition [8-31].

The histogram modification technique is the most common method available in image contrast enhancement, which expands the histogram using a transfer function [9]. The transfer function can be used in the global or local mode. In the global mode, the transfer function is calculated based on all gray levels in the histogram, while in the local mode, the transfer function is obtained from a special interval of histogram [10-13]. Histogram Equalization is a well-known method in the global contrast enhancement. Histogram equalization

uses a transfer function based on cumulative distribution of all intensities in the image. Histogram equalization is not suitable for keeping the mean brightness of the image, and causes intensity saturation problems [14]. In [14], Kim has proposed a method called BBHE, which is based upon histogram equalization on each one of the two sub-histograms that are separated by the mean value. In the output images of the BBHE method, the over-enhanced regions can be seen due to the application of only one separation on the histogram. In [15], Wang has presented a method called DSIHE. In this method, in the first step, the histogram is divided into two equal sub-histograms based on the middle value of gray levels. Then the histogram equalization is applied to each sub-histogram. Since DSIHE divides the histogram into just two sub-histograms, this method has the same problem of BBHE. In order to overcome this problem, Sim presented the RSIHE method in [16] based on DSIHE. The RSIHE method, in a recursive operation, divides the histogram of the image into two equal sub-histograms. This operation is repeated for  $r$  times.

The histogram is divided into  $2r$  sections, and then the histogram equalization is applied for each sub-histogram. A large  $r$  is suitable for preserving mean brightness but there is no special enhancement. With a small  $r$ , this method operates similar to DSIHE.

In [25], the bi-histogram equalization plateau limit (BHEPL) has been proposed to control the BBHE enhancement rate. BBHE applies a higher stretching process to the contrast of the high-histogram regions and compresses the contrast of the low histogram regions, possibly causing intensity saturation in the low histogram regions. A clipping process is applied to each sub-histogram of BBHE to deal with the intensity saturation problem and to control the enhancement rate through setting the plateau limit as the average number of intensity occurrence. If the bins for any intensity exceed the plateau limit, they are replaced by the plateau limit level; otherwise, they remain the same as the original bins of the input histogram. Finally, HE is implemented to the clipped sub-histograms.

In [17], Draa has proposed a method based on finding the best transfer function using the Artificial Bee Colony (ABC) algorithm with a fitness function based on entropy and Sobel operator. In [21], Pourya Hoseini has proposed a hybrid algorithm including Genetic Algorithm (GA), Ant Colony Optimisation (ACO), and Simulated Annealing (SA) metaheuristics for increasing the contrast of images. Ant colony optimization is used to generate the transfer functions, which map the input intensities to the output one. Simulated annealing, as a local search method, is utilized to modify the transfer functions generated by ant colony optimization. Genetic algorithm has the responsibility of evolutionary process of ants' characteristics.

In [18], Khan has proposed a method based on the local histogram equalization. In this method, the image histogram is divided into several parts according to the middle and mean values. The narrow areas of the histogram are then discovered and are expanded to a full brightness area, like in the HE method.

After equalization of every part with the HE method, the image is normalized in order to prevent the brightness saturation issues. In [19], Huang has proposed a method in which, according to the mean value of image, the histogram is divided into several parts, and the histogram equalization is then applied for each part. In this method, after histogram equalization, the image details would be lost due to some large divisions and lots of changes in brightness.

In [24], Huang has proposed a combinatorial method, which contains the gamma correction and the traditional histogram equalization. This method has created a balance between a high level of visual quality and a low computational cost.

Gu [26] has used saliency preserving to increase the image contrast without dealing with the artifact problem. The proposed framework includes the histogram equalization and its relevant visual pleasing conducted by the sigmoid function. Finally, this method exploits a quality determination measure based upon saliency preserving to automatically select parameters.

In [27], a method has been proposed to avoid over-enhancement and noise addition, while improving the contrast of an image. The method is a combination of Contrast Limit Adaptive Histogram Equalization (CLAHE) and Discreet Wavelet Transform (DWT). High frequencies of the image and its low counterparts are first decomposed by DWT. The image frequency coefficients are equalized by CLAHE, while leaving image high frequency with no alteration. Eventually, the reverse DWT is employed to reconstruct the image. In the last step, a weighted factor is obtained from the original and the enhanced image to control the possible over-enhancement.

Estimating and compressing the illumination component is a good method to enhance the degraded images by an uneven light. In [28], Liang has proposed a novel method to estimate the illumination by an iterative solution of non-linear diffusion equation.

In [29], Celik has proposed a new algorithm to enhance images using special information of pixels. This algorithm computes the spatial entropy of pixels by considering the distribution of spatial locations of gray levels.

In the proposed method, which is based on [19], the histogram is divided into several optimal parts according to density, mean, and standard deviation of image intensities. Then the large sections are identified and again divided into several parts. Finally, the enhanced image is constructed with local histogram equalization. The results obtained show that this method not only keeps the pixel mean and features but also enhances the image contrast.

## 2. Proposed method

One of the common methods used for enhancing image contrast is an approach based on histogram modification. These methods map image pixels aiming at expanding image histogram using a transfer function. The transfer function used for

enhancing image contrast can be in two modes; global and local. In the global mode, the transfer function is calculated in proportion to the entire histogram. In the local mode, this transferring function is applied for a special interval of histogram. The proposed method is divided into two parts.

The first part is histogram division, and the histogram is divided into parts to calculate the transfer function locally. The second part is the local equalization of histogram. One of the famous methods used for contrast enhancement is the histogram equalization method. Histogram equalization produces an image whose density levels of brightness are uniform, resulting in an increase in the pixel intervals, which has a considerable effect on the image quality. In this part, the actions of histogram equalization in local mode are discussed.

### 2.1. Histogram division

In this part, the image histogram is divided according to diffusion of the existing brightness levels in the image. If the brightness values for the image are in the [a,b] interval,  $H(i)$ ,  $i = a, a + 1, a + 2, \dots, b$ , indicates the number of image pixels with an  $i$  brightness level. In fact,  $H$  is the histogram function of the image brightness level. Based on this, the mean and standard deviation of the image brightness value are calculated using (1) and (2).

$$\mu = \frac{\sum_{i=a}^b H(i) * i}{\sum_{i=a}^b H(i)} \quad (1)$$

$$\sigma = \left( \frac{1}{\left( \sum_{i=a}^b H(i) \right) - 1} \sum_{i=a}^b H(i) (i - \mu)^2 \right)^{1/2} \quad (2)$$

The algorithm of histogram division is:

Algorithm 1: Suppose that the brightness level value of image is in [0,255].

- In the first step, initialize  $a = 0$  and  $b = 255$ .
- Mean and standard deviation of image are calculated in [a,b].
- Two threshold values to separate and divide the histogram are calculated by (3) and (4).

$$T_1 = \mu - \sigma \quad (3)$$

$$T_2 = \mu + \sigma \quad (4)$$

- Now,  $[a, T_1]$  and  $[T_2, b]$  are two parts of the histogram that are stored.
- In this step, to divide  $[T_1, T_2]$  into smaller parts, we replace the pixels values of the image that were in  $[a, T_1]$  with mean pixel value of  $[a, T_1]$ . Also we replace the pixel values of the image in

$[T_2, b]$  with the mean pixels value of  $[T_2, b]$  ((5) and (6)).

$$\frac{\sum_{i=a}^{T_1} i * H(i)}{T_1 - a} \quad (5)$$

$$\frac{\sum_{i=T_2}^b i * H(i)}{b - T_2} \quad (6)$$

- Put the “a” value equal to  $T_1 + 1$  and “b” equal to  $T_2 - 1$ , and repeat the algorithm from step 2. The stopping criterion of this loop is that the difference between the image PSNR criteria for two successive steps would be more than 0.1. Otherwise, this image can be still divided into smaller intervals. 0.1 is obtained experimentally. PSNR is most commonly used to measure the quality of reconstruction of lossy compression codecs. Since histogram division is a kind of compression, and has less complexity, we use the PSNR measure to compute the similarity of two images. PSNR is a criterion that shows the ratio between the peak possible power of signal and the noise failure power and its effects on displaying signal. In fact, it calculates the similarity of two images, and its value is calculated as follows ((7) and (8)).

$$PSNR = 20 * \log_{10} \frac{255}{RMSE} \quad (7)$$

$$RMSE = \left( \frac{1}{MN} \sum_{x=0}^{M-1} \sum_{y=0}^{N-1} [I'_{xy} - I_{xy}]^2 \right)^{1/2} \quad (8)$$

$I$  and  $I'$  show the mean level of the original and enhanced image with  $M*N$  pixels. RMSE is the root of mean square error, and is calculated from the difference between the estimated values by the model and real observed values. The output of this step is shown in figure 1. In the  $i$ 'th step of applying algorithm 1, where  $i = 1, 2, \dots, t$ , the two  $[a^{(i)}, T_1^{(i)}]$  and  $[T_2^{(i)}, b^{(i)}]$  intervals are stored in  $S$  matrix.  $t$  is a step, in which the difference value of PSNR between  $t$  and  $t-1$  is greater than 0.1, and  $S$  matrix indicates dividing intervals of the histogram in algorithm 1. Different steps of algorithm 1 are shown in a diagram in figure 8a. Figure 4 shows the divided histogram and obtained intervals with algorithm 1 for figure 9a. In this figure,  $t$  or steps of algorithm would be equal to 3.

As it can be seen in figure 4, based on density, mean, and standard deviation, algorithm 1 divides the histogram into intervals but some of the selected intervals, which are shown in figure 4 with arrows, have covered a vast scope of the histogram. This causes an increasing brightness value change in these intervals in the local

histogram equalization step, failure to maintain image mean, and loss of some image features (Figure 5). As specified in figure 5, in great intervals (two intervals have been shown), the brightness changes are too much and the image details would disappear (shown in the results section).

$$\begin{bmatrix} a^{(1)} & T_1^{(1)} \\ a^{(2)} & T_1^{(2)} \\ \vdots & \vdots \\ a^{(t)} & T_1^{(t)} \end{bmatrix}, \begin{bmatrix} T_2^{(1)} & b^{(1)} \\ \vdots & \vdots \\ T_2^{(2)} & b^{(2)} \\ \vdots & \vdots \\ T_2^{(t)} & b^{(t)} \end{bmatrix} \rightarrow S = \begin{bmatrix} a^{(1)} & T_1^{(1)} \\ a^{(2)} & T_1^{(2)} \\ \vdots & \vdots \\ a^{(i)} & T_1^{(i)} \\ T_1^{(i)+1} & T_2^{(i)}-1 \\ T_2^{(i)} & b^{(i)} \\ \vdots & \vdots \\ T_2^{(2)} & b^{(2)} \\ T_2^{(t)} & b^{(t)} \end{bmatrix}$$

Figure 1. intervals obtained from implementation of algorithm 1.

In order to overcome this problem, it is necessary to prevent the creation of great intervals. Considering a constant value of p as a threshold value for each pair of consecutive intervals in S that has a difference greater than p is a solution. Algorithm1 can again be applied for the original (input) image. However, the stopping condition, PSNR criterion, should be greater than 0.1 in the two consecutive algorithm steps and the difference between a and b should be greater than the threshold value for p in each step. Thus:

- If the difference between  $T_1^{(i)}$  and  $a^{(i)}$ ,  $i = 1, 2, \dots, t$ , is greater than p, algorithm 1 in step 2 starts with the values  $a = a^{(i)}$  and  $b = T_1^{(i)}$ , and the intervals obtained, like the structure in figure 1, would be added to the new T set. Otherwise,  $[a^{(i)}, T_1^{(i)}]$  would be added to the T set.
- The  $[T_1^{(i)+1}, T_2^{(i)}-1]$  interval is added to the T set.
- Accordingly, for the second section of S, if the difference between  $b^{(i)}$  and  $T_2^{(i)}$ ,  $i = 1, 2, \dots, t$ , is greater than p, algorithm 1 of step 2 is carried out with starting values of  $a = T_2^{(i)}$  and  $b = b^{(i)}$ , and the intervals obtained with structures like that in figure 1 would be added to the T set; otherwise,  $[T_2^{(i)}, b^{(i)}]$  would be added to the T set.

After this procedure with p parameter greater than 50, the histogram intervals of figure 9a would be as in figure 6. As observed, with re-implementation of algorithm 1, the intervals greater than 50 in figure 4 are divided into smaller intervals, based on mean and variance (Figure 6).

This procedure causes the mean brightness pixels to be more preserved after the histogram local equalization, which is applied for each interval.

Figure 7 shows that selecting smaller intervals causes histogram uniformity, and the mean brightness of pixels is completely preserved (enhanced image is shown in the results section). In figure 8b, the diagram of steps of re-division of histogram by algorithm 1 and the place of histogram equalization are shown. In order to determine the optimum value for the PSNR threshold and “p”, four images were analyzed. Figure 2 shows the PSNR threshold to number of sub-histograms ratio. For values greater than 0.1, the number of sub-histograms does not change too much.

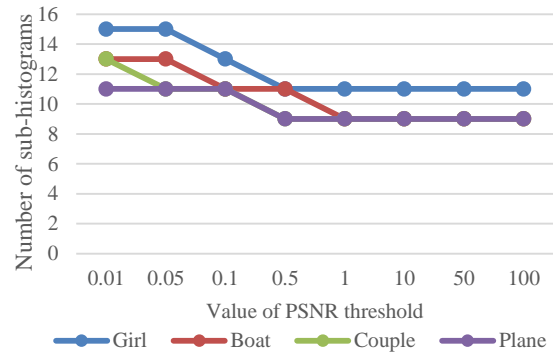


Figure 2. PSNR threshold to number of sub-histograms ratio.

Figure 3 shows the “p” value to number of sub-histograms greater than “p” ratio. For values bigger than 50, the number of sub-histograms greater than “p” reaches zero, which makes the proposed method ineffective.

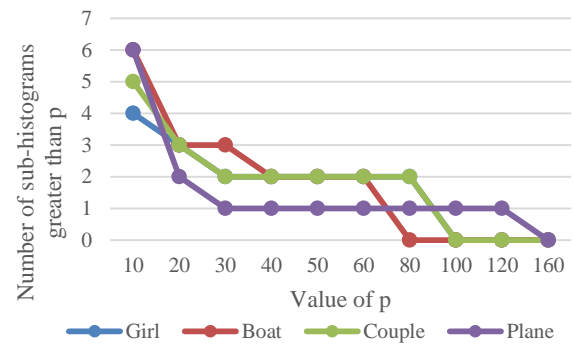


Figure 3. Value of “p” to number of sub-histogramm greater than “p” ratio.

## 2.2. Local Equalization of Histogram

Up to this point, image histogram is partitioned into parts, and the existing intervals are obtained in set T. We will save the number of produced intervals via the previous step algorithm, in e parameter.

The method of histogram local equalization is as follows:

First, for each  $e$  interval of the histogram, in the original (input) image, the probability density function is calculated based on (9).

$$pdf^k(i) = \frac{n_i}{\sum_i n_i} \quad (9)$$

$k = 1, 2, \dots, e,$

$i = T(k,1), T(k,1)+1, T(k,1)+2, \dots, T(k,2)$

$i$  is the brightness level in the  $k$ 'th interval; the first index of the  $T$  set shows row, and the second index shows column.  $n_i$  also shows the number of  $i$  brightness levels in the original image. Also the cumulative distribution function (CDF) is calculated for each part of the histogram in the original image by (10).

$$cdf^k(i) = \sum_{h=T(k,1)}^i pdf^k(h) \quad (10)$$

$k = 1, 2, \dots, e,$

$i = T(k,1), T(k,1)+1, T(k,1)+2, \dots, T(k,2)$

$i$  is the brightness level in the  $k$ 'th interval; the first index of the  $T$  set shows row, and the second index shows column. Using a mapping function, and applying  $k$ 'th cdf on the  $k$ 'th interval of the original image (sub-image), we will reach the enhanced image with (11).

$$P^k(i) = T(k,1) + (T(k,2) - T(k,1)) * cdf^k(i) \quad (11)$$

$k = 1, 2, \dots, e,$

$i = T(k,1), T(k,1)+1, T(k,1)+2, \dots, T(k,2)$

$P^k(i)$ , in fact, is the histogram value in the  $k$ 'th interval of brightness level of  $i$  in the original image.

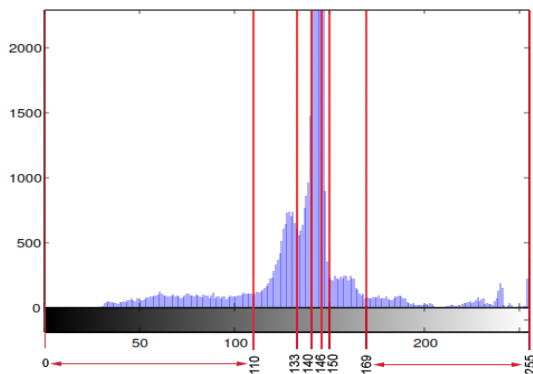


Figure 4. Histogram divisions and the obtained intervals by initial implantation of algorithm 1.

### 3. Results

In this part, the proposed methods will be compared with the other methods. The results of test with parameter  $p = 50$  were evaluated in two cases.

#### 3.1. Qualitative evaluation

Different contrast enhancement algorithms are evaluated for four famous image visually. Figure

9a shows the image that the histogram equalization algorithm is applied to, where there are lots of inconsistencies among background, hair, body, and face in the two original and enhanced images. Results of the BBHE, DSIHE, and RSIHE algorithms are shown in figure 9c, figure 9f, and figure 9b, respectively. These methods use the local sub-histograms for decreasing the histogram equalization effect but many result aspects still exist as a result of applying the histogram equalization in these methods. For example, hair and clothes are rather dark, face is too bright, there are lots of changes in the pixel brightness values, and therefore, lots of image details have been lost.

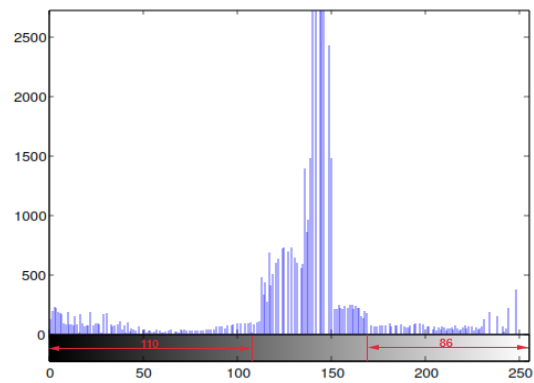


Figure 5. Results of applying local histogram equalization on initial intervals by algorithm 1 on Figure 9a.

$$T = \begin{bmatrix} 0 & 54 \\ 55 & 96 \\ 97 & 110 \\ 111 & 133 \\ 134 & 140 \\ \mathbf{141} & \mathbf{145} \\ 146 & 149 \\ 150 & 168 \\ 169 & 183 \\ 184 & 194 \\ 195 & 236 \\ 237 & 241 \\ 242 & 255 \end{bmatrix} [T_1^{(t)} + 1 \quad T_2^{(t)} - 1]$$

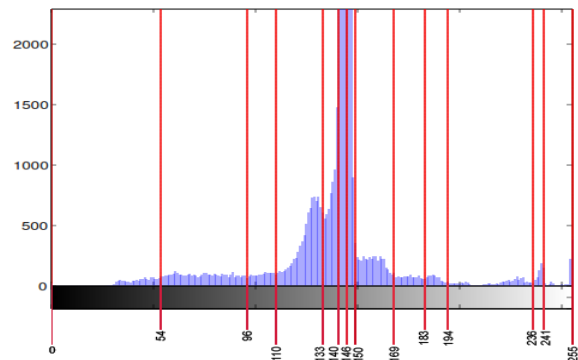
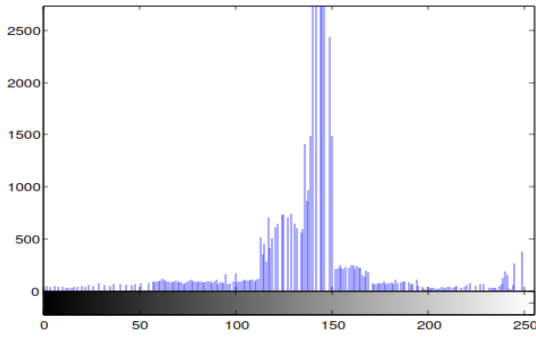


Figure 6. Histogram divisions and intervals obtained on Figure 9a after re-implantation of algorithm 1 for intervals larger than  $p$ .



**Figure 7. Result of local histogram equalization on secondary intervals formed by re-implantation of algorithm 1 on Figure 9a.**

In figure 9g, the results of applying algorithm [19] can be seen where somehow the mean of image brightness is preserved and great enhancement is applied. However, due to the long length of some intervals, some image details have been lost; for example, hair area is completely dark.

In figure 9i, the result of SDDMHE method is shown, which is not enhanced enough. In figure 9h, the enhanced image from the proposed algorithm has been shown. Because of using the local sub-histograms with optimum intervals, in addition to enhanced contrast, the mean value of pixels is preserved, and therefore, none of the image details have been lost; for example, hair area seems more natural. Also figure 9d shows the result of the ABC method that presents the same enhanced results with the proposed method, except the bow tie and face area. Also in figures 10 and 11, the proposed ABC and RSIHE methods; and in figure 12, the proposed method generate the best output image.

If you choose not to use this document as a template, prepare your technical work in single-spaced, double-column format. Set bottom margins to 25 millimeters (0.98 inch) and top, left and right margins to about 20 millimeters (0.79 inch). Margin of First page is different from other pages. For first page set top margin to 30 millimeters (1.18 inch), and bottom, left and right margins are similar to other pages. Do not violate margins (i.e., text, tables, figures, and equations may not extend into the margins). The column width is 78 millimeters (3.07 inches). The space between the two columns is 13 millimeters (0.51 inch).

### 3.2. Quantitative evaluation

In addition to the qualitative evaluation, measuring the accuracy is one of the requirements to compare the proposed method and the other existing methods.

There are five measuring criteria used in this paper: PSNR, AMBE [20], FSIM [22], KL[30] distance, and DE [23].

AMBE is the absolute difference between the mean values of input image X and output image Y to define the normalized absolute mean brightness error (12) ( $AMBE \in [0,1]$ ).

$$AMBE(X, Y) = \frac{1}{1 + |MB(X) - MB(Y)|} \quad (12)$$

where,  $MB(X)$  and  $MB(Y)$  are the average values of X and Y, respectively. In table 1, the AMBE values for the contrast enhancement methods are shown on 10 images. The proposed ABC and SDDMHE methods can completely preserve the mean values of image pixels because they use the local histogram equalization with optimum intervals instead of the global histogram equalization. Therefore, they can effectively decrease AMBE. Table 2 shows the PSNR values obtained by applying a different algorithm on the previous images. We can see that the PSNR values obtained by the proposed method have maximum values. A greater PSNR value indicates that there is more similarity between the original and enhanced images. Histogram equalization refers to processing the input image to utilize the dynamic range efficiently by mapping an input into output image such that there is an equal number of pixels at each grey-level in the output. Thus it is expected that the equalized output image has flattened the grey-level distribution. However, it should be noted that the process should not change the overall shape of the input histogram to protect the image content. In order to quantitatively measure how flattened the output grey-level distribution is, the Kullback–Leibler (KL) distance between the distribution of the processed output image  $p(y_k)$  and the uniform distribution  $q(y_k)$  was used. The KL-distance (13) is a natural distance function from a “true” probability distribution,  $p(y_k)$ , to a “target” probability distribution,  $q(y_k)$ .

$$KL(p, q) = \sum_{v_k} p(y_k) \log_2 \left( \frac{p(y_k)}{q(y_k)} \right) \quad (13)$$

The lower the value of KL, the better the histogram equalization is. Table 3 shows that the proposed method output generates the lowest KL-distance between other methods.

Another quantitative evaluation is the discrete entropy (DE). The discrete entropy of the input image X with K distinct grey-levels is in (14).

$$DE(X) = -\sum_{k=1}^K p(x_k) \log p(x_k) \quad (14)$$

where,  $p(x_k)$  is the probability of pixel intensity  $x_k$ , which is estimated from the normalized histogram. Similarly, the discrete entropy of the output image  $Y_w$  with  $L$  distinct grey-levels is defined as (15).

$$DE(Y_w) = -\sum_{i=1}^L p(y_i) \log p(y_i) \quad (15)$$

where,  $p(y_i)$  is the probability of pixel intensity  $y_i$ . A higher value of  $DE$  indicates that the image has richer details. Using the metrics  $DE(X)$  and  $DE(Y_w)$ , the normalized discrete entropy ( $DE_N(X, Y_w) \in [0, 1]$ ) between the input image  $X$  and the output image  $Y_w$  is defined as (16).

$$DE_N(X, Y_w) = \frac{1}{1 + \frac{(\log(256) - DE(Y_w))}{(\log(256) - DE(X))}} \quad (16)$$

where,  $\log(256)$  is the maximum value of entropy that can be achieved using the 8-bits data representation. The higher the value of normalized discrete entropy, the better the enhancement is in terms of utilizing the dynamic range and providing better image details. Table 4 shows the  $DE$  value for different algorithms.

The visual information in an image is often very redundant, while HVS understands an image mainly based on its low-level features.

**Table 1. Comparing various methods with AMBE.**

Test Images	HE	BBHE	DSIHE	[21]	[19]	Proposed	RSIHE	SDD MHE	ABC
<b>baboon</b>	0.0673	0.0796	0.0652	0.3382	0.0813	0.1816	0.1383	<b>0.4077</b>	0.1296
<b>boat</b>	0.0447	0.3169	0.0213	0.3637	0.0708	<b>0.4878</b>	0.2756	0.1442	0.3584
<b>City</b>	0.0145	0.0503	0.0137	0.0347	0.1267	<b>0.5220</b>	0.1599	0.3816	0.2209
<b>Couple</b>	0.1884	0.1051	0.1092	0.3665	0.2765	<b>0.9831</b>	0.3293	0.6331	0.6260
<b>Girl</b>	0.0565	0.0474	0.0390	0.1007	0.2899	<b>0.6501</b>	0.2898	0.4218	0.3858
<b>Jet</b>	0.0194	0.3142	0.1232	0.0473	0.1490	<b>0.4975</b>	0.1566	0.2983	0.2002
<b>Lenna</b>	0.2249	0.1146	0.3467	0.1416	0.1313	<b>0.9657</b>	0.2057	0.6089	0.4375
<b>Man</b>	0.0252	0.0400	0.0220	0.0445	0.1204	0.2735	0.1325	1.3892	<b>0.9874</b>
<b>Peppers</b>	0.0599	0.1392	0.1615	0.2256	0.1665	0.3582	0.1467	<b>0.4971</b>	0.2245
<b>Plan</b>	0.0205	0.3762	0.1197	0.0315	0.3680	<b>0.4284</b>	0.2349	0.2148	0.1977
<b>Average</b>	0.0721	0.1584	0.1022	0.1694	0.1780	<b>0.5348</b>	0.2069	0.4997	0.3768

**Table 2. Comparing various methods with PSNR.**

Test Images	HE	BBHE	DSIHE	[21]	[19]	Proposed	RSIHE	SDD MHE	ABC
<b>baboon</b>	18.23	18.56	13.97	22.20	26.24	<b>30.80</b>	23.64	27.64	18.91
<b>boat</b>	17.97	18.14	13.08	18.56	24.13	<b>32.83</b>	32.82	31.13	18.47
<b>City</b>	11.03	16.38	10.50	15.58	20.64	<b>32.92</b>	22.66	29.85	20.90
<b>Couple</b>	17.22	17.26	14.20	17.69	22.59	<b>30.58</b>	28.10	28.10	17.55
<b>Girl</b>	13.85	14.60	17.77	16.68	20.15	<b>35.16</b>	30.12	30.28	23.96
<b>Jet</b>	12.84	21.91	16.87	18.82	27.32	<b>34.28</b>	26.04	28.43	21.89
<b>Lenna</b>	20.13	20.15	21.95	24.01	28.98	27.33	25.23	<b>31.23</b>	24.63
<b>Man</b>	16.53	19.09	14.38	19.84	23.28	<b>34.03</b>	25.38	18.14	18.03
<b>Peppers</b>	20.35	21.75	21.13	26.85	<b>31.36</b>	26.18	26.21	30.55	21.20
<b>Plan</b>	10.23	14.29	19.02	13.20	18.80	<b>36.09</b>	33.66	31.28	27.90
<b>Average</b>	15.84	18.21	16.29	19.34	24.35	<b>32.02</b>	27.39	29.66	21.34

**Table 3. Comparing various methods with KL.**

Test Images	HE	BBHE	DSIHE	[21]	[19]	Proposed	RSIHE	SDD MHE	ABC
<b>baboon</b>	2.0242	1.6299	0.7356	0.7242	0.7142	<b>0.3449</b>	0.7736	0.9156	0.7613
<b>boat</b>	2.0464	2.1224	1.0737	1.0394	0.9349	<b>0.4332</b>	1.004	1.1302	0.5865
<b>City</b>	2.0721	1.7622	1.2515	1.2133	1.1363	0.9895	1.1606	1.4986	<b>0.5757</b>
<b>Couple</b>	2.0408	1.5532	1.0101	0.9909	0.9307	<b>0.5226</b>	0.9379	1.1099	0.7561
<b>Girl</b>	3.1498	3.8185	2.8002	2.5443	2.4394	<b>1.7853</b>	2.5175	2.7288	2.1528
<b>Jet</b>	2.2886	2.0348	1.4453	1.4004	1.4258	<b>0.7586</b>	1.4959	1.7674	4.4943
<b>Lenna</b>	2.0307	1.2927	0.73	0.659	0.6627	0.4748	0.6915	0.8386	<b>0.2135</b>
<b>Man</b>	2.0486	1.065	0.709	0.7335	0.638	<b>0.3984</b>	0.6771	0.6962	0.6952
<b>Peppers</b>	2.0267	0.6835	0.6313	0.6029	0.595	0.6256	0.6197	0.7135	<b>0.4291</b>
<b>Plan</b>	4.2533	4.2304	4.32	4.0942	4.0119	<b>3.0112</b>	4.0353	3.9958	3.0218
<b>Average</b>	2.3981	2.0193	1.4707	1.4002	1.3489	<b>0.9344</b>	1.3913	1.5395	1.3686

In other words, the salient low-level features convey crucial information for HVS to interpret the scene. Accordingly, perceptible image

degradations will lead to perceptible changes in image low-level features, and hence, a good IQA metric could be devised by comparing the low-

level feature sets between the reference image and the distorted image. Based on the physiological and psychophysical evidence, the visually discernable features coincide with the points where the Fourier waves at different frequencies have congruent phases, i.e. at points of high phase congruency (PC), we can extract highly informative features. Therefore, PC is used as the primary feature in computing FSIM. Meanwhile, considering that PC is contrast invariant but image local contrast does affect HVS' perception on the image quality, the image gradient magnitude (GM) is computed as the secondary feature to encode contrast information. PC and GM are complementary, and they reflect different aspects of HVS in assessing the local quality of the input image. After computing the local similarity map, PC is utilized again as a weighting function to derive a single similarity score. Suppose that we are going to calculate the similarity between images  $f_1$  and  $f_2$ . Denote by  $PC_1$  and  $PC_2$  the PC maps extracted from  $f_1$  and  $f_2$ , and  $G_1$  and  $G_2$ , the GM maps extracted from them. It should be noted that for color images, the PC and GM features are extracted from their luminance channels. FSIM is defined and computed based on  $PC_1$ ,  $PC_2$ ,  $G_1$ , and  $G_2$ . Computation of the FSIM index consists of two stages. In the first stage, the local similarity map is computed, and then in the second stage, we pool the similarity map into a single similarity score. We separate the feature similarity measurement between  $f_1(x)$  and  $f_2(x)$  into two components, each for PC or GM. First, the similarity measure for  $PC_1(x)$  and  $PC_2(x)$  is defined as (17).

$$S_{PC}(X) = \frac{2PC_1(x).PC_2(x) + T_1}{PC_1^2(x) + PC_2^2(x) + T_1} \quad (17)$$

where,  $T_1$  is a positive constant to increase the stability of  $S_{PC}$ . Similarly, the GM values  $G_1(x)$  and  $G_2(x)$  are compared, and the similarity measure is defined as (18).

$$S_G(x) = \frac{2G_1(x).G_2(x) + T_2}{G_1^2(x) + G_2^2(x) + T_2} \quad (18)$$

where,  $T_2$  is a positive constant depending on the dynamic range of the GM values. In our experiments, both  $T_1$  and fixed to all databases so that the proposed FSIM can be conveniently used. Then  $S_{PC}(x)$  and  $S_G(x)$  are combined to get the similarity  $S_L(x)$  of  $f_1(x)$  and  $f_2(x)$ . We define  $S_L(x)$  as (19).

$$S_L(x) = S_{PC}(x).S_G(x) \quad (19)$$

Having obtained the similarity  $S_L(x)$  at each location  $x$ , the overall similarity between  $f_1$  and  $f_2$  can be calculated.

However, different locations have different contributions to the HVS perception of the image. For example, the edge locations convey more crucial visual information than the locations within a smooth area. Since the human visual cortex is sensitive to the phase congruent structures, the PC value at a location can reflect how likely it is a perceptibly significant structure point. Intuitively, for a given location  $x$ , if anyone of  $f_1(x)$  and  $f_2(x)$  has a significant PC value, it implies that this position  $x$  will have a high impact on HVS in evaluating the similarity between  $f_1$  and  $f_2$ . Therefore, we use  $PC_m(x)$  to weight the importance of  $S_L(x)$  in the overall similarity between  $f_1$  and  $f_2$ , and accordingly, the FSIM index between  $f_1$  and  $f_2$  is defined as (20) and (21).

$$PC_m(x) = \max(PC_1(x), PC_2(x)) \quad (20)$$

$$FSIM = \frac{\sum_{x \in \Omega} S_L(x).PC_m(x)}{\sum_{x \in \Omega} PC_m(x)} \quad (21)$$

As specified in table 5, the proposed RSIHE and the ABC method generate the best FSIM values, respectively.

**Table 4. Comparing various methods with DE.**

Test Images	HE	BBHE	DSIHE	[21]	[19]	Proposed	RSIHE	SDD MHE	ABC
<b>baboon</b>	0.2341	0.2751	0.4568	0.4607	0.4641	<b>0.6102</b>	0.4443	0.4032	0.5483
<b>boat</b>	0.2832	0.2759	0.4296	0.4376	0.4505	<b>0.6512</b>	0.4461	0.4171	0.4638
<b>City</b>	0.3259	0.3624	0.4446	0.4522	0.4572	0.4685	0.4633	0.4006	<b>0.535</b>
<b>Couple</b>	0.1968	0.2685	0.4261	0.4391	0.4544	<b>0.6937</b>	0.4377	0.3846	0.4616
<b>Girl</b>	0.4208	0.3747	0.4497	0.4735	0.4827	<b>0.5617</b>	0.4762	0.4561	0.484
<b>Jet</b>	0.3599	0.3873	0.4709	0.4788	0.4626	<b>0.5997</b>	0.4624	0.4213	0.4743
<b>Lenna</b>	0.2146	0.3003	0.4319	0.4571	0.4513	<b>0.6221</b>	0.4452	0.3982	0.4558
<b>Man</b>	0.1886	0.309	0.4018	0.3937	0.4066	0.4066	<b>0.4429</b>	0.4062	0.4274
<b>Peppers</b>	0.1806	0.3952	0.4143	0.4256	0.4165	<b>0.5757</b>	0.4188	0.385	0.4288
<b>Plan</b>	0.4844	0.4857	0.4805	0.4939	0.499	0.499	0.4975	0.5	<b>0.6432</b>
<b>Average</b>	0.2889	0.3434	0.4406	0.4512	0.4545	<b>0.5688</b>	0.4534	0.4172	0.4922

**Table 5. Compare various method with FSM.**

Test Images	HE	BBHE	DSIHE	[21]	[19]	Proposed	RSIHE	SDD MHE	ABC
<b>baboon</b>	0.8395	0.9365	0.8936	0.9571	0.9449	<b>0.9929</b>	0.9194	0.8947	0.9194
<b>boat</b>	0.6859	0.8236	0.8077	0.9208	0.8889	<b>0.9933</b>	0.9829	0.8728	0.983
<b>City</b>	0.7566	0.8328	0.7893	0.9173	0.8858	0.9863	<b>0.9907</b>	0.8407	0.9382
<b>Couple</b>	0.8938	0.8205	0.8137	0.9044	0.8838	<b>0.9895</b>	0.9577	0.8192	0.9577
<b>Girl</b>	0.5737	0.6302	0.5986	0.7161	0.8377	<b>0.9732</b>	0.962	0.6521	0.9692
<b>Jet</b>	0.8464	0.8744	0.7514	0.9595	0.9196	0.9795	<b>0.9965</b>	0.9185	0.9648
<b>Lenna</b>	0.9112	0.9576	0.9284	0.9729	0.9328	<b>0.99</b>	0.9561	0.9321	0.9561
<b>Man</b>	0.9165	0.9377	0.9486	0.947	0.9521	0.9874	<b>0.9889</b>	0.9366	0.9599
<b>Peppers</b>	0.9476	0.967	0.9479	0.9798	0.9709	<b>0.99</b>	0.9595	0.9454	0.9603
<b>Plan</b>	0.5057	0.6026	0.5681	0.7403	0.9066	0.9708	<b>0.9777</b>	0.6207	0.9773
<b>Average</b>	0.7877	0.8383	0.8047	0.9015	0.9123	<b>0.9853</b>	0.9691	0.8433	0.9586

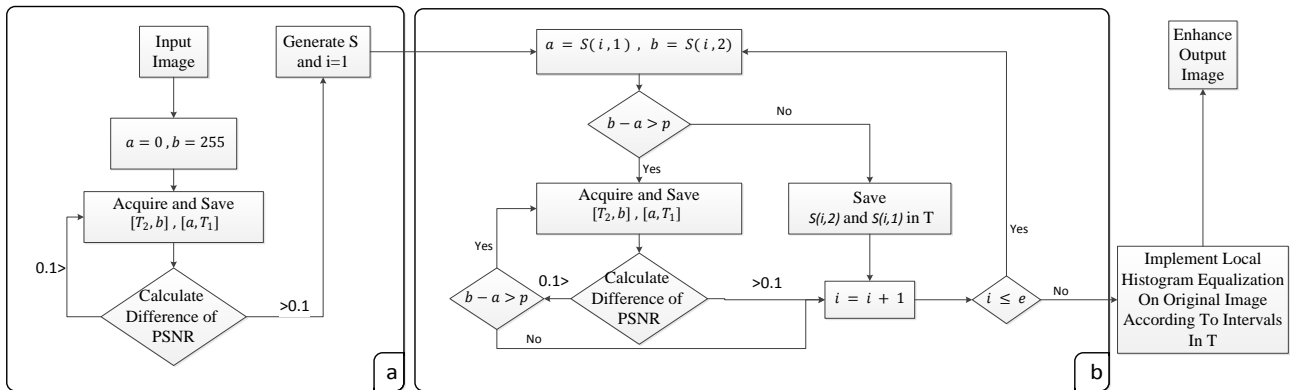


**Figure 8. (a) Algorithm 1 steps (b) steps of re-implantation of algorithm 1 for intervals. larger than p.**



**Figure 9. Girl (a) The original Image, The experimental image under study (b) The enhanced image by Histogram Equalization (c) The enhanced image by BBHE (d) The enhanced image by ABC (e) the enhanced image by RSIHE (f) The enhanced image by DSIHE (g) The enhanced image by the proposed method (h) The enhanced image by SDDMHE (i) The enhanced image by SDDMHE (j) The enhanced image by [21].**

**4. Conclusion**

In this paper, a new method was proposed for image contrast enhancement without losing image details. Intensity saturation and over-enhancement is one of the main issues in the other proposed contract enhancement methods. In order to overcome this problem and also to obtain a desired contrast enhancement, the image histogram is first divided into some sub-histograms according to the mean value and standard deviation. Then every single sub-

histogram is enhanced separately using the traditional histogram equalization. Finally, these enhanced sub-histograms are combined to make the enhanced image. The qualitative and quantitative results of comparing different contrast enhancement methods with the proposed method show that the proposed method not only keeps the details and image brightness level mean but also enhances the image contrast effectively, and leads to an increased image quality. Selecting the parameters related to the number of sub-

histograms was one of the problems faced with in this work. A solution is using a method to obtain

the value of “p” and PSNR threshold according to the input image.

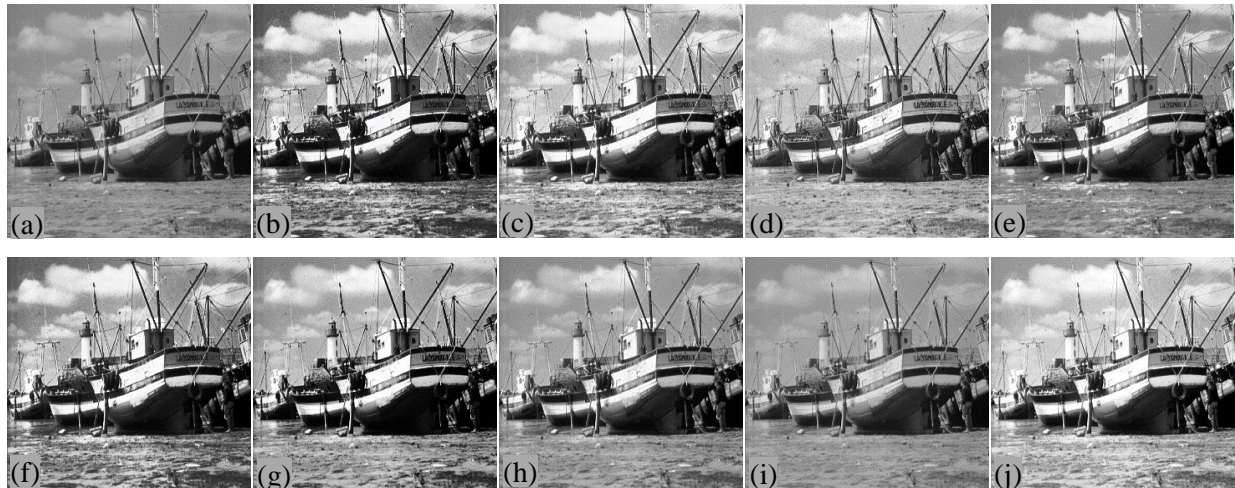


Figure 10. Boat (a) Original Image (b) Enhanced image by Histogram Equalization (c) Enhanced image by BBHE (d) Enhanced image by ABC (e) Enhanced image by RSIHE (f) Enhanced image by DSIHE (g) Enhanced image by [19] (h) Enhanced image by proposed method (i) Enhanced image by SDDMHE (j) Enhanced image by [21].



Figure 11. Couple (a) Original Image (b) Enhanced image by Histogram Equalization (c) Enhanced image by BBHE (d) Enhanced image by ABC (e) Enhanced image by RSIHE (f) Enhanced image by DSIHE (g) Enhanced image by [19] (h) Enhanced image by proposed method (i) Enhanced image by SDDMHE (j) Enhanced image by [21].

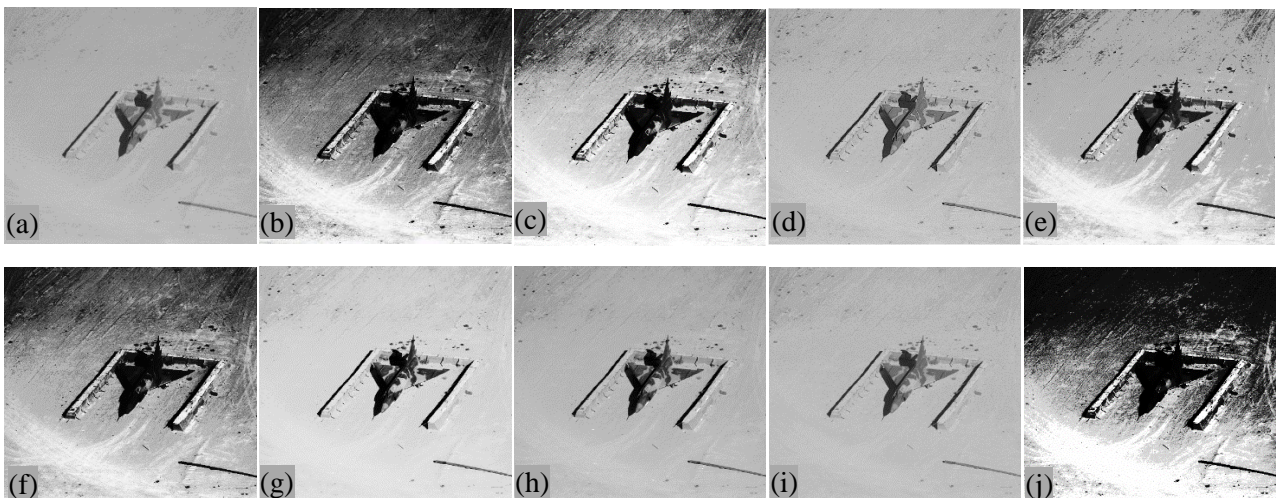


Figure 12. Plan (a) Original Image (b) Enhanced image by Histogram Equalization (c) Enhanced image by BBHE (d) Enhanced image by ABC (e) Enhanced image by RSIHE (f) Enhanced image by DSIHE (g) Enhanced image by [19] (h) Enhanced image by proposed method (i) Enhanced image by SDDMHE (j) Enhanced image by [21].

## References

- [1] Chen, C. Y., Lin, T. M., & Wolf, W. H. (2008). A visible/infrared fusion algorithm for distributed smart cameras. *IEEE Journal of Selected Topics in Signal Processing*, vol. 2, no. 4, pp. 514-525.
- [2] Lai, C. C., & Tsai, C. C. (2008). Backlight power reduction and image contrast enhancement using adaptive dimming for global backlight applications. *IEEE Transactions on Consumer Electronics*, vol. 54, no. 2, pp. 669-674.
- [3] Kim, Y. T. (1997). Contrast enhancement using brightness preserving bi-histogram equalization. *IEEE transactions on Consumer Electronics*, vol. 43, no. 1, pp. 1-8.
- [4] Kim, J. Y., Kim, L. S., & Hwang, S. H. (2001). An advanced contrast enhancement using partially overlapped sub-block histogram equalization. *IEEE transactions on circuits and systems for video technology*, vol. 11, no. 4, pp. 475-484.
- [5] Wang, Y., Chen, Q., & Zhang, B. (1999). Image enhancement based on equal area dualistic sub-image histogram equalization method. *IEEE Transactions on Consumer Electronics*, vol. 45, no. 1, pp. 68-75.
- [6] Sim, K. S., Tso, C. P., & Tan, Y. Y. (2007). Recursive sub-image histogram equalization applied to gray scale images. *Pattern Recognition Letters*, vol. 28, no. 10, pp. 1209-1221.
- [7] Xie, X., & Lam, K. M. (2005). Face recognition under varying illumination based on a 2D face shape model. *Pattern Recognition*, vol. 38, no. 2, pp. 221-230.
- [8] van Bommel, C. M., Wink, O., Verdonck, B., Viergever, M. A., & Niessen, W. J. (2003). Blood pool contrast-enhanced MRA: improved arterial visualization in the steady state. *IEEE transactions on medical imaging*, vol. 22, no. 5, pp. 645-652.
- [9] Arici, T., Dikbas, S., & Altunbasak, Y. (2009). A histogram modification framework and its application for image contrast enhancement. *IEEE Transactions on image processing*, vol. 18, no. 9, pp. 1921-1935.
- [10] Abdullah-Al-Wadud, M., Kabir, M. H., Dewan, M. A. A., & Chae, O. (2007). A dynamic histogram equalization for image contrast enhancement. *IEEE Transactions on Consumer Electronics*, vol. 53, no. 2, pp. 593-600.
- [11] Lamberti, F., Montrucchio, B., & San, A. (2006). CMBFHE: A novel contrast enhancement technique based on cascaded multistep binomial filtering histogram equalization. *IEEE Transactions on Consumer Electronics*, vol. 52, no. 3, pp. 966-974.
- [12] Chen, Z., Abidi, B. R., Page, D. L., & Abidi, M. A. (2006). Gray-level grouping (GLG): an automatic method for optimized image contrast Enhancement-part I: the basic method. *IEEE transactions on image processing*, vol. 15, no. 8, pp. 2290-2302.
- [13] Chen, S. D., & Ramli, A. R. (2003). Contrast enhancement using recursive mean-separate histogram equalization for scalable brightness preservation. *IEEE Transactions on Consumer Electronics*, vol. 49, no. 4, pp. 1301-1309.
- [14] Kim, Y. T. (1997). Contrast enhancement using brightness preserving bi-histogram equalization. *IEEE transactions on Consumer Electronics*, vol. 43, no. 1, pp. 1-8.
- [15] Wang, Y., Chen, Q., & Zhang, B. (1999). Image enhancement based on equal area dualistic sub-image histogram equalization method. *IEEE Transactions on Consumer Electronics*, vol. 45, no. 1, pp. 68-75.
- [16] Sim, K. S., Tso, C. P., & Tan, Y. Y. (2007). Recursive sub-image histogram equalization applied to gray scale images. *Pattern Recognition Letters*, vol. 28, no. 10, pp. 1209-1221.
- [17] Draa, A., & Bouaziz, A. (2014). An artificial bee colony algorithm for image contrast enhancement. *Swarm and Evolutionary computation*, vol. 16, pp. 69-84.
- [18] Khan, M. F., Khan, E., & Abbasi, Z. A. (2014). Segment dependent dynamic multi-histogram equalization for image contrast enhancement. *Digital Signal Processing*, vol. 25, pp. 198-223.
- [19] Huang, S. C., & Yeh, C. H. (2013). Image contrast enhancement for preserving mean brightness without losing image features. *Engineering Applications of Artificial Intelligence*, vol. 26, no. 5, pp. 1487-1492.
- [20] Kim, M., & Chung, M. G. (2008). Recursively separated and weighted histogram equalization for brightness preservation and contrast enhancement. *IEEE Transactions on Consumer Electronics*, vol. 54, no. 3, pp. 1389-1397.
- [21] Hoseini, P., & Shayesteh, M. G. (2013). Efficient contrast enhancement of images using hybrid ant colony optimisation, genetic algorithm, and simulated annealing. *Digital Signal Processing*, vol. 23, no. 3, pp. 879-893.
- [22] Zhang, L., Zhang, L., Mou, X., & Zhang, D. (2011). FSIM: a feature similarity index for image quality assessment. *IEEE transactions on Image Processing*, vol. 20, no. 8, pp. 2378-2386.
- [23] Shannon, C. E. (2001). A mathematical theory of communication. *ACM SIGMOBILE Mobile Computing and Communications Review*, vol. 5, no. 1, pp. 3-55.
- [24] Huang, S. C., Cheng, F. C., & Chiu, Y. S. (2013). Efficient contrast enhancement using adaptive gamma correction with weighting distribution. *Image Processing, IEEE Transactions on*, vol. 22, no. 3, pp. 1032-1041.
- [25] Ooi, C. H., Kong, N. S. P., & Ibrahim, H. (2009). Bi-histogram equalization with a plateau limit for digital image enhancement. *IEEE Transactions on*

Consumer Electronics, vol. 55, no. 4, pp. 2072-2080.

[26] Gu, K., Zhai, G., Yang, X., Zhang, W., & Chen, C. W. (2015). Automatic contrast enhancement technology with saliency preservation. *IEEE Transactions on Circuits and Systems for Video Technology*, vol. 25, no. 9, pp. 1480-1494.

[27] Lidong, H., Wei, Z., Jun, W., & Zebin, S. (2015). Combination of contrast limited adaptive histogram equalisation and discrete wavelet transform for image enhancement. *IET Image Processing*, vol. 9, no. 10, pp. 908-915.

[28] Liang, Z., Liu, W., & Yao, R. (2016). Contrast Enhancement by Nonlinear Diffusion Filtering. *IEEE Transactions on Image Processing*, vol. 25, no. 2, pp. 673-686.

[29] Celik, T. (2014). Spatial entropy-based global and local image contrast enhancement. *IEEE Transactions on Image Processing*, vol. 23, no. 12, pp. 5298-5308.

[30] Kullback, S., & Leibler, R. A. (1951). On information and sufficiency. *The annals of mathematical statistics*, vol. 22, no. 1, pp. 79-86.

[31] Shafeipour Yourdeshahi, S., Seyedarabi, H., & Aghagolzadeh, A. (2016). Video-based face recognition in color space by graph-based discriminant analysis. *Journal of AI and Data Mining*, vol. 4, no. 2, pp. 193-201.

## تقسیم‌بندی هیستوگرام مبتنی بر چگالی و تعدیل محلی به منظور بهبود کنتراست تصویر

محسن شاکری، میرحسین دزفولیان و حسن ختن لو\*

گروه مهندسی کامپیوتر، دانشگاه بوعلی سینا، همدان، ایران.

ارسال ۲۰۱۶/۰۱/۱۰؛ پذیرش ۲۰۱۷/۰۴/۰۸

### چکیده:

تکنیک تعدیل هیستوگرام یکی از پایه‌ای‌ترین روش‌های موجود برای بهبود کنتراست تصویر است. استفاده از این روش در تصاویری که دارای سطوح خاکستری یکنواختی هستند (هیستوگرام باریک) باعث از دست رفتن جزئیات تصویر شده و ظاهر طبیعی آن را از بین می‌برد. به‌منظور پوشش این مشکل یک روش دومرحله‌ای در این مقاله ارائه شده است. در مرحله اول، هیستوگرام تصویر با توجه به مقادیر میانگین و انحراف معیار به زیر بخش‌هایی تقسیم می‌شود، که با مقدار PSNR کنترل خواهد شد. در مرحله دوم، هر یک از زیر بخش‌ها به‌صورت جداگانه و محلی بهبود داده می‌شوند. در آخر نیز زیر بخش‌ها با یکدیگر ترکیب شده و تصویر بهبود داده‌شده به دست خواهد آمد. نتایج تجربی نشان می‌دهد که این روش نه‌تنها ظاهر طبیعی تصویر را حفظ می‌کند بلکه جزئیات تصویر را نیز بهبود می‌بخشد.

**کلمات کلیدی:** بهبود کنتراست، تصحیح هیستوگرام، ارزیابی کیفیت تصویر، بهبود کیفیت تصویر.